JOURNAL OF SOLID STATE CHEMISTRY **131,** 341–349 (1997)
ARTICLE NO. SC977392

Structural and Thermodynamic Characterization of the Perovskite-Related $Ba_{1+y}UO_{3+x}$ and $(Ba, Sr)_{1+y}UO_{3+x}$ Phases

E. H. P. Cordfunke, A. S. Booij, V. Smit-Groen, and P. van Vlaanderen

Netherlands Energy Research Foundation ECN, P. O. Box 1, 1755 ZG Petten, The Netherlands

and

D. J. W. IJdo

Gorlaeus Laboratories, Leiden Institute of Chemistry, Leiden University, P. O. Box 9502, 2300 RA Leiden, The Netherlands

Received November 18, 1996; in revised form March 10, 1997; accepted March 12, 1997

The perovskite-type $BaUO_3$ structure has been investigated by X-ray and neutron diffraction. The Ba/U ratio, the (Ba, Sr)/U ratio, and the oxygen stoichiometry in $Ba_{1+y}UO_{3+x}$ were varied, and the integral enthalpies of formation were determined by solution calorimetry. In addition, equilibrium oxygen partial pressures were measured using a reversible EMF cell. The chemical defect mechanism is discussed, and it is shown that the continuous series $BaUO_3$–$Ba_{1+y}UO_{3+x}$–Ba_3UO_6 exists in which uranium vacancies are gradually filled with barium ions whereas uranium is oxidized via the pentavalent to the hexavalent state in Ba_3UO_6 (=$Ba_2(Ba, U)O_6$). © 1997 Academic Press

1. INTRODUCTION

Complex actinide oxides with one or more metal ions in addition to the actinide ions are of interest because they can be formed during fission in nuclear fuel. Thus, the so-called "grey phase" is formed as inclusions in highly irradiated UO_2 or $(U,Pu)O_2$ fuel. This phase has the perovskite-type ABO_3 structure and contains, besides the cations on the *A* sites (barium and strontium), on the *B* sites uranium and elements such as plutonium and zirconium. Its general formula is (Ba, Sr, Cs) (U, Pu, Zr, Mo,)O_3 (1).

The fission products strontium and barium exhibit different behavior in irradiated fuels. Whereas the oxide of strontium is predominantly dissolved in UO_2, the majority of barium is precipitated in the grey phase (2, 3). A knowledge of the chemical state of these fission products in irradiated fuels is of importance for an understanding of the fuel performance and for their behavior under accident circumstances. To this purpose a series of investigations was carried out in our laboratories to characterize the ABO_3-type perovskites, with A = Ba and Sr and B = U. In a previous paper we reported a study of the perovskite-type strontium uranate (4). Instead of $SrUO_3$, a new phase with the formal composition $Sr_2UO_{4.5}$ was found with a statistical distribution of Sr and U^{5+} on one of the octahedral positions and one U^{5+} on the other position, leading to the formula $Sr_2(Sr_{2/3}U_{1/3})UO_6$. Ternary oxides ABO_3 (A = alkaline earth metal and B = actinide metal) have been studied by many authors (5–8), and the various aspects related to thermal stability and defect mechanisms have been discussed. In the present study the $BaUO_3$ structure was investigated in which both the Ba/U ratio and the oxygen stoichiometry were varied. In addition, partial replacement of barium by strontium was studied with the aim of clarification of the difference in behavior of barium and strontium in these perovskite-type structures.

2. EXPERIMENTAL

The starting materials for the preparation of $BaUO_3$ were BaO and UO_2. The latter compound was prepared by reduction of U_3O_8 in hydrogen at 700°C, and BaO was prepared by decomposition of $BaCO_3$ (purified from strontium by recrystallization of the starting material $Ba(NO_3)_2$, Baker p.a.) in a gold boat in high vacuum at 1000°C. SrO was prepared by decomposition of $SrCO_3$ (Baker, p.a.) in high vacuum at temperatures which were gradually increased to 1050°C. The alkaline earth uranates were prepared in X/U ratios (X = Ba or (Ba + Sr)) that varied from 1.0 to 3.0 by heating the purified oxides in an (argon + hydrogen) atmosphere at a temperature of 950°C followed by heating the samples at 1300°C. Since the BaO in the samples reacts with both gold and platinum, it was necessary to heat them as pellets on already reacted pellets in crucibles of stabilized ZrO_2. After the heatings the samples were stored in a glove box filled with dried argon.

0022-4596/97 $25.00

The chemical analyses were carried out after dissolution of the sample in HCl and separation of the alkaline earths by an ion exchanger. Total U was determined titrimetrically with dichromate. In the case of only Ba the content of the alkaline earth was determined complexometrically with EDTA; in the case of two different alkaline earth metals the analyses were done with AES. All handlings of the samples. including the weighing, were carried out in an argon-filled CO_2-free dry glove box. The oxygen content of $BaUO_{3+x}$ was determined from the weight increase by ignition of the sample in oxygen to $BaUO_4$; $Ba_{1+y}UO_{3+x}$ was determined from the analyzed Ba/U ratio, and the weight increase was obtained by oxidizing the samples in oxygen at 1000°C to $Ba_3UO_6 + BaUO_4$.

Density measurements were done picnometrically with double-distilled CCl_4. To achieve a satisfactory accuracy, large samples (~ 5 g) were used in the determinations in a picnometer with a content of 25 cm^3. To avoid trapped voids in the polycrystalline samples, the picnometer was filled in vacuum; the measurements were done in triplicate.

The X-ray diffraction patterns were made on single-coated film with a focusing Guinier camera (FR 552, Enraf Nonius, Delft, The Netherlands) using $CuK\alpha_1$ radiation ($\lambda = 1.5405981(3)$ Å) with α-SiO_2 (hexagonal, $a = 4.9133(2)$, $c = 5.4053(4)$ Å) as an internal standard.

The neutron diffraction measurements were taken on the powder diffractometer at the HFR in Petten. Neutrons with $\lambda = 2.57176(3)$ Å were obtained using the beam reflected from the *hkl* (111) planes of a single crystal of copper, reducing the λ/n contamination to less than 0.1% by means of a pyrolitic graphite filter. Soller slits with a horizontal divergence of 30′ were placed between the reactor and the monochromator and in front of the four ^{3}He counters. The sample holder (diameter 1.43 cm) consisted of a V tube closed with Cu plugs fitted with O rings. The diffraction pattern was taken at 300 K and analyzed by means of Rietveld's profile refinement technique (9). Absorption corrections were applied according to Weber (10). For the coherent scattering lengths we used the values for O 5.805, Ba 5.07, Sr 7.02, and U 8.417 fm (11). For the refinement of the neutron diffraction data the program DBW 9006, version 8.491, was used (12). The variables include a scale factor, five background parameters, three half-width parameters defining the Gaussian-like peak shape, the counter zero, an asymmetry parameter, the unit cell dimensions, atomic position parameters, and thermal parameters. A scale factor for the small contribution of the V sample holder was also refined. Three samples were studied by neutron diffraction, namely $BaUO_{3.05}$, $Ba_{1.553}UO_{3.866}$, and $(Ba_{0.92}Sr_{0.23})UO_{3.45}$.

The enthalpies of formation of $BaUO_{3+x}$ and $Ba_{1+y}UO_{3+x}$ at 298.15 K were obtained from their enthalpies of solution in 0.77 *M* HCl(+ $FeCl_3$) as measured in an isoperibol solution calorimeter at 298.15 K. The details of the calorimetric measurements have been described elsewhere (13).

The electromotive force (EMF) measurements were carried out, using a Keithley 617 electrometer, with a zirconia tube as the electrolyte, and separated electrode compartments. Temperature measurements were done with calibrated Pt/Pt, Rh(10%) thermocouples.

3. RESULTS

Synthesis of $Ba_{1+y}UO_{3+x}$

Attempts to prepare $BaUO_{3+x}$ with a Ba/U ratio of 1.0 were unsuccessful. In all cases a trace of UO_2 was found as a secondary phase. A monophasic barium uranate was obtained at Ba/U ratios > 1, and it appeared that a solubility limit for barium in excess was obtained at Ba/U ratios > 2.0 under the conditions of the synthesis (low oxygen pressures; see experimental). At higher ratios BaO was present as a secondary phase. As expected, the volume of the unit cell increases with increasing Ba content until the solubility limit is reached. Figure 1 shows the relationship between the volume of the pseudo-cubic "$BaUO_3$" cell and the Ba/U ratio. The results are given in Table 1 with the O/U ratio of the samples.

Synthesis of $(Ba, Sr)_{1+y}UO_{3+x}$

To study the influence of the replacement of Ba by Sr ions on the $BaUO_3$ structure, samples containing (Ba + Sr)/U ratios up to 2.0 were prepared by heating mixtures of BaO, SrO, and UO_2 under the same conditions as described for $BaUO_3$. It appeared to be possible to dissolve a little less than 1.0 mol SrO in the $BaUO_3$ structure, which resulted in a slight decrease of the cell volume (Fig. 1). At the ratio (Ba + Sr)/U = 2.0 some SrO was present as the second phase. As discussed in a previous paper (4), it is not possible to obtain $SrUO_3$; the compound $Sr_2UO_{4.5}$ is formed instead. It appeared possible to dissolve BaO in this phase (Table 2); it is to be expected that the larger Ba ions will be situated on the *A* sites, where more space is available than on the *B* sites.

Structure Determinations

The structure of $BaUO_{3.05}$ could be refined with space group *Pbnm*, analogous to $BaPuO_3$(14). The agreement with the observed and calculated profiles is shown in Fig. 2a. The data given in Tables 3a and 3b exhibit regular UO_6 octahedra, as in $BaPuO_3$, which is, however, in disagreement with the earlier results of Barrett *et al.* (6). Barrett *et al.* assumed Ba vacancies to be present but from our neutron diffraction data it is not possible to discriminate between uranium and barium vacancies. The X-ray powder diffraction data of a second sample $Ba_{1.553}UO_{3.866}$

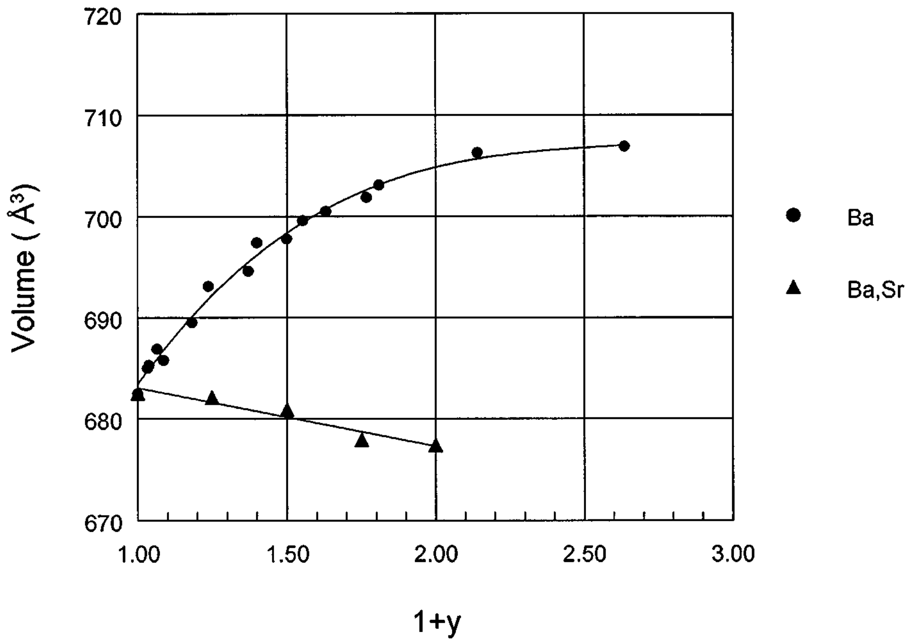

FIG 1. The unit cell volume of Ba$_{1+y}$UO$_{3+x}$ and (Ba, Sr)$_{1+y}$UO$_{3+x}$ as a function of the Ba/U ratio (●) or the (Ba, Sr)/U ratio (▲).

(= Ba(Ba$_{0.207}$ U$_{0.777}$)O$_3$) indicate a nearly cubic face-centered unit cell (a = 8.8 Å), but refinement of the neutron powder diffraction data with space group *Fm*3*m*, with U and (U + Ba) in octahedral positions, failed. Refinement in space group *Pnma* analogous to BaUO$_3$ also failed, but refinement in space group $R\bar{3}$ gave better results (Tables 4a and 4b). The simultaneous occupancy of one octahedral site by U and the other by (U + Ba) introduces a considerable disorder in the structure which cannot easily be modelled. As a consequence, only an average structure can be determined. A significant improvement was obtained when the statistic disorder was represented by anisotropic oxygen thermal parameters. It should be noted that the transition from a pseudo-cubic to a rhombohedral structure is only evident from the neutron diffraction work. The structure of (Ba$_{0.92}$Sr$_{0.23}$)UO$_{3.45}$ could be refined with space group *Pbnm* analogous to BaUO$_{3+x}$ (Tables 5a and 5b). It has been assumed that in the compound, which can also be described as Ba$_{0.80}$Sr$_{0.08}$(Sr$_{0.13}$U$_{0.87}$)O$_3$, no vacancies are present in the *A* positions and in the O lattice; this is confirmed by density measurements (see Discussion). The agreement with the observed and calculated profiles is shown in Fig. 2b.

TABLE 1
Oxygen Contents and Cell Volumes of Ba$_{1+y}$UO$_{3+x}$ Phases

(Ba/U ratio) (1 + y)	x	Phases (P, perovskite)	Cell volume (Å^3)[a]
1.033	0.135–0.133	P	685.0
1.038		P	685.3
1.040		P + tr.UO$_2$	
1.065	0.163–0.181	P	686.9
1.086		P	685.8
1.182		P	689.5
1.238	0.417–0.397	P	693.1
1.371		P	694.6
1.400	0.595–0.613	P	697.4
1.499		P	697.8
1.553	0.864–0.867	P	699.6
1.631		P	700.5
1.766		P	701.9
1.809		P	703.1
2.140		P	706.3
2.635		P + BaO	706.9

[a] Cell volume calculated with a cubic cell with 2a_0, obtained from the Guinier measurements.

TABLE 2
(Ba, Sr)UO$_{3+x}$ Compositions and Cell Volumes of Equilibrium Phases

Sample	Phase	Cell volume (Å^3)
BaSr$_{0.25}$UO$_{3+x}$	BaUO$_3$	682.1
BaSr$_{0.50}$UO$_{3+x}$	BaUO$_3$	680.9
BaSr$_{0.75}$UO$_{3+x}$	BaUO$_3$	677.9
BaSr$_{1.00}$UO$_{3+x}$	BaUO$_3$ + SrO	677.4
Sr$_2$(Sr$_{0.67}$U$_{0.33}$)UO$_6$	Sr$_2$UO$_{4.5}$	640.7
Sr$_{1.50}$Ba$_{0.5}$(Sr$_{0.5}$U$_{0.4}$$\square_{0.1}$)UO$_6$	Sr$_2$UO$_{4.5}$	653.7
Sr$_{1.33}$Ba$_{0.67}$(Sr$_{0.67}$U$_{0.33}$)UO$_6$	Sr$_2$UO$_{4.5}$ + SrO	657.9

TABLE 3a
Fractional Atomic Coordinates and Isotropic Thermal Parameters of $Ba_{0.99}U_{0.99}O_3$ ($Pbnm$)

	x	y	z	B (Å^2)	Occupation
Ba	0.9975(14)	0.0224(10)	0.25	1.25(10)	0.988(6)
U	0	0.5	0	0.25(5)	0.989(5)
O(1)	0.0699(10)	0.4966(12)	0.25	0.92(15)	1.0
O(2)	0.7266(9)	0.2735(9)	0.0389(5)	1.93(11)	1.0

Note. $a = 6.2590(7)$ Å, $b = 6.2397(5)$ Å, $c = 8.8123(8)$ Å, $V = 344.16(6)$ Å^3, $\rho_{calc} = 8.087$ g/cm^3, $R_p = 3.37$, $R_{wp} = 4.57$, $S = 1.71$, $D\text{–}wD = 0.91$.

The Enthalpies of Formation of $Ba_{1+y}UO_{3+x}$

The enthalpies of formation of five different barium uranate compositions were calculated from the enthalpy-of-solution data listed in Table 6, according to the reaction scheme given for one of the compositions, $Ba_{1.033}UO_{3.134}$, in Table 7. The reference data for reactions 2 through 8 have been taken from recent publications by Cordfunke *et al.* (15, 16). In Table 8 the enthalpies of formation of all samples are listed with data for $Ba_2U_2O_7$ and Ba_3UO_6 (17). A recent third-law evaluation of mass-spectrometric measurements of the dissociation pressures of $BaUO_{3.12}$, to give BaO(g) and UO_2(18), yields for the enthalpy of formation $\Delta_f H°(298.15\,K) = -1742.5 \pm 16.5\,kJ\,mol^{-1}$ in perfect agreement with the calorimetric results.

As expected, there is a linear correlation between the enthalpy of formation and the Ba/U ratio (Fig. 3), from which it is possible to extrapolate the enthalpy of formation of "$BaUO_3$" with a Ba/U ratio of 1.0 and $x = 0$: $\Delta_f H°(298.15\,K) = -(1680 \pm 10)\,kJ\,mol^{-1}$. This value is in good agreement with previous determinations (5). As will be discussed later in this paper, the correlation is valid over the whole range from $BaUO_3$, in which uranium has the formal valency of 4+, to Ba_3UO_6, in which uranium is 6+.

TABLE 3b
Atomic Distances (Å) and Angles (°) in $Ba_{0.99}U_{0.99}O_3$ at Room Temperature

Ba–O(1)	2.712(11)	U–O(1)	2.246(1)
Ba–O(1)	2.993(10)	–O(2)	2.245(6)
Ba–O(1)	3.312(10)	–O(2)	2.246(6)
Ba–O(2)	2.800(8) 2×	O(1)–U–O(2)	90.4(2)
	2.965(8) 2×	O(1)–U–O(2)	91.1(2)
	3.187(7) 2×	O(2)–U–O(2)	91.5(2)
		U–O(1)–U	157.5(3)
		U–O(2)–U	159.5(2)

The Oxygen Potential of $BaUO_{3+x}$

The thermodynamic stability of $BaUO_{3+x}$ has been determined by measuring the oxygen potential of a reversible electromotive cell of the type

$$(-)(Pt)BaUO_{3+x}|ZrO_2|O_2(Pt)(+)$$

in which ZrO_2 is a calcia-stabilized ZrO_2 tube which is closed at one side. The EMF cell has separated electrodes, with the reference electrode O_2 at a fixed pressure (air, $pO_2 = 0.2$ atm) and a sintered pellet of $Ba_{1+y}UO_{3+x}$ in an argon/CO (20%) atmosphere as the second electrode. Since the latter electrode is monophasic, the equilibrium

$$\tfrac{1}{2}O_2(g) + 2e = O^{2-}$$

is a function of x in $Ba_{1+y}UO_{3+x}$ at a constant temperature. This can be measured either by coulometric titration or by analysis of the equilibrium composition at a certain temperature. Because the oxygen potential of $BaUO_{3+x}$ is very low near the stoichiometric composition, slight oxidation of the uranate via the gas phase always occurs, resulting in a slow drift of the EMF. For that reason we preferred to measure the EMF of the cell as a function of x in $BaUO_{3+x}$ at a fixed temperature. After each equilibrium measurement the composition was analyzed, as described before; the composition $Ba_{1.033}UO_{3.13}$ was taken as the starting material. When the equilibrium composition was reached, the cell was rapidly cooled and the composition determined by chemical analysis. It was assumed that during cooling the composition did not change. It was checked that the results of the EMF measurements at a certain composition were reversible and reproducible. To that purpose a sample of $Ba_{1.033}UO_{3+x}$ was measured as a function of temperature increase and decrease, and the composition was determined after the measurements. The equilibrium was always attained rapidly. The results of the EMF measurements at three different temperatures are collected in Table 9. We thus obtain at 1060 K $E(mV) = 1595.9 - 1138.2 \cdot x$ and at 1090 K $E(mV) = 1494.6 - 874.8 \cdot x$. The partial oxygen pressures for the various x values calculated from these EMF values are listed in Table 9 and shown in Fig. 4.

4. DISCUSSION

Attempts to prepare stoichiometric $BaUO_{3.00}$ have always been unsuccesful; such samples always contain a very small amount of UO_2 as a secondary phase. This has been found before (5, 6, 8) and is confirmed by the results of

FIG. 2. Observed (dots) and calculated (full line) neutron diffraction profiles of (a) $BaUO_{3.05}$ and (b) $(Ba_{0.92}Sr_{0.23})UO_{3.45}$ $[Ba_{0.92}Sr_{0.08}$ $[Sr_{0.13}U_{0.87}]O_3]$. Tick marks below the profiles indicate the positions of the Bragg reflections. Difference (observed − calculated) curves appear at the bottom of the plots. Two theta in degrees.

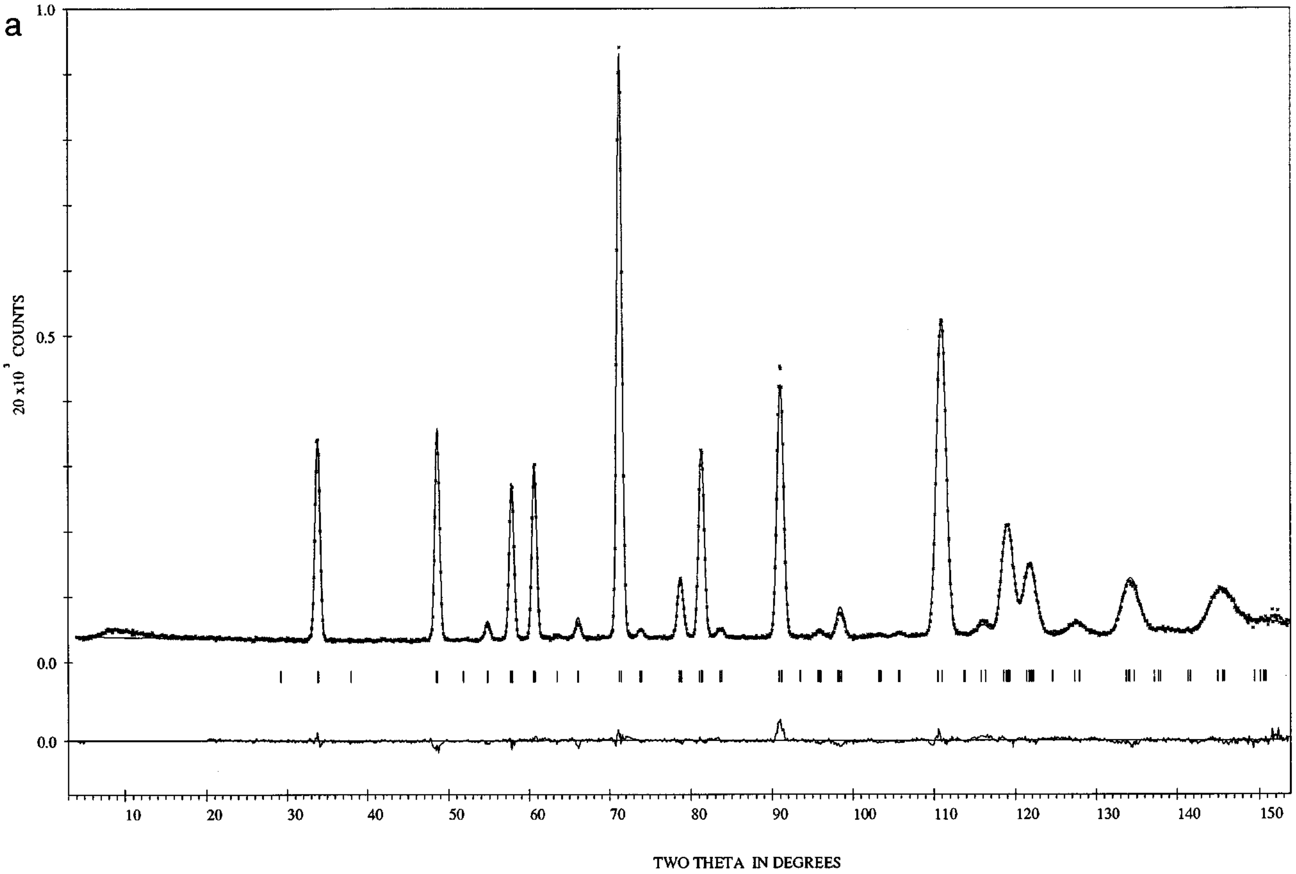
a
1.0
0.5
0.0
0.0
20 x10³ COUNTS
10
20
30
40
50
60
70
80
90
100
110
120
130
140
150
TWO THETA IN DEGREES

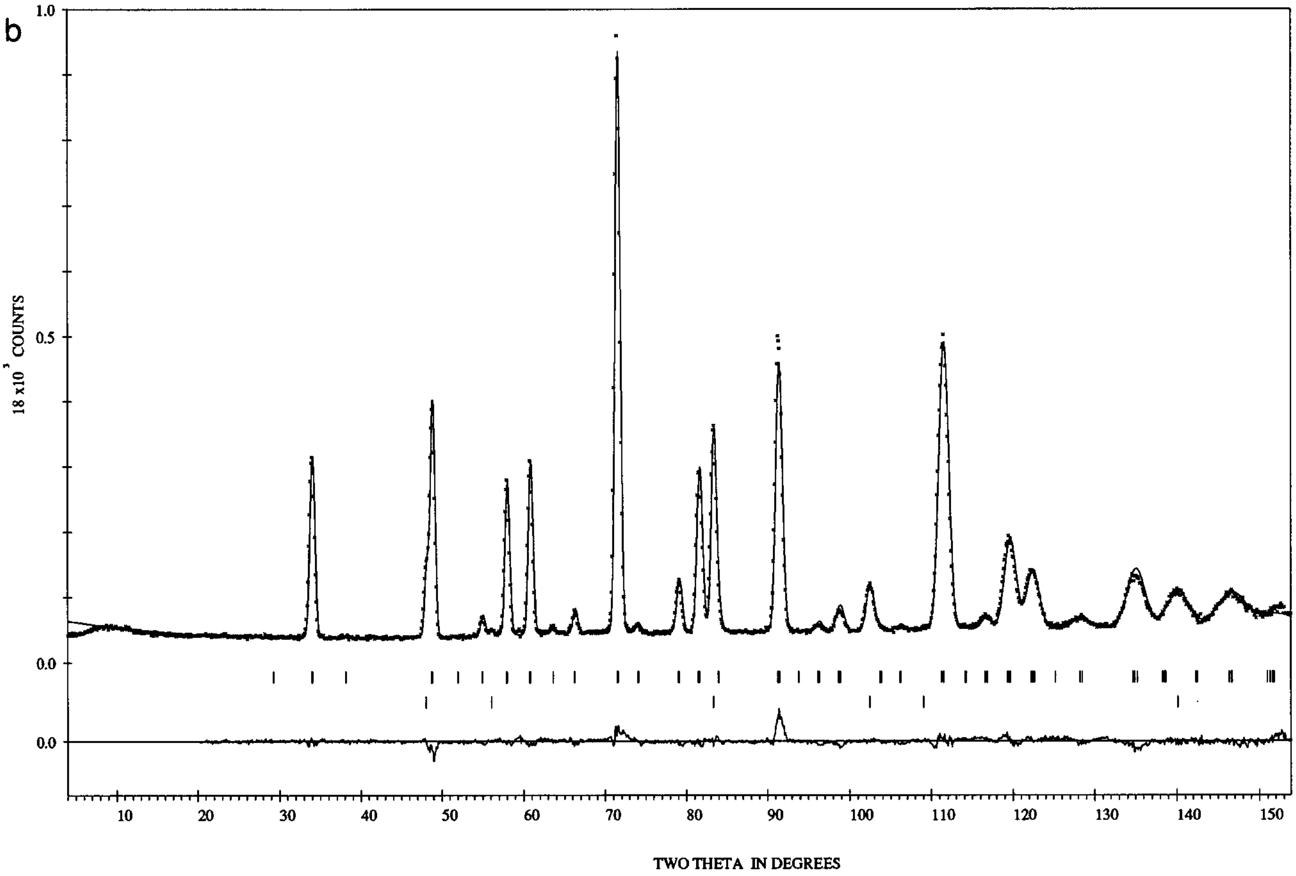
b
1.0
0.5
0.0
0.0
18 x10³ COUNTS
10
20
30
40
50
60
70
80
90
100
110
120
130
140
150
TWO THETA IN DEGREES

TABLE 4a
Fractional Atomic Coordinates and Isotropic Thermal Parameters of $Ba_2(Ba_{0.414}U_{0.554})UO_6$ ($R\bar{3}$)

Atom	x	y	z	B(Å^2)	Occupation
Ba(1)	0.2456(22)	x	x	2.10(13)	1.0
U(1)	0	0	0	1.13(7)	1.0
Ba(2)	0.5	0.5	0.5	1.13	0.414
U(2)	0.5	0.5	0.5	1.13	0.554
O(1)	−0.2418(25)	0.1839(9)	0.2931(7)	3.2	1.0

Note. $a = 6.2713(6)$ Å, $\alpha = 60.165(8)$, $R_p = 4.24$, $R_{wp} = 5.37$, $S = 3.41$, $D\text{–}wD = 0.26$, $\rho_{calc} = 7.563$ g/cm^3, $\rho_{exp} = 7.55$ g/cm^3.

TABLE 5a
Fractional Atomic Coordinates and Isotropic Thermal Parameters of $Ba_{0.92}Sr_{0.08}(Sr_{0.13}U_{0.87})O_3$ ($Pbnm$)

	x	y	z	B(Å^2)
Ba/Sr	0.9968(24)	0.0248(3)	0.25	1.30(10)
U/Sr	0	0.5	0	0.65(6)
O(1)	0.0753(19)	0.4897(18)	0.25	2.50(6)
O(2)	0.7242(16)	0.2747(17)	0.0370(7)	2.50(6)

Note. $a = 6.2344(11)$ Å, $b = 6.2245(8)$ Å, $c = 8.7949(13)$ Å, $V = 341.30(11)$ Å^3, $\rho_{calc} = 7.780$ g/cm^3, $\rho_{exp} = 7.77$ g/cm^3, $R_p = 3.87$, $R_{wp} = 5.00$, $S = 1.92$, $D\text{–}wD = 0.77$.

the present study. The equilibrium oxygen potential of stoichiometric $BaUO_{3.00}$ (~ -615 kJ mol^{-1}; see Table 9 and Fig. 4) is not only low enough to cause some dissociation of BaO to Ba(g), but also too low to be maintained during the preparation, and uptake of oxygen into the lattice will take place, either during the synthesis or during handling in the glove box. Thus, the phase $BaUO_{3.08}$ (Table 8) can be described as $Ba_{0.974}U_{0.974}O_3$, in which 2.6% of the uranium positions are empty, and as having an equivalent number of Ba and U vacancies. By addition of BaO the vacancies are gradually filled. In $Ba_{1.033}UO_{3.134}$ ($= Ba_{0.99}U_{0.957}O_3$) the uranium vacancies amount to 4.3%. In agreement here are the densities of $BaUO_{3.08}$ ($Ba_{0.974}U_{0.974}O_3$) and $Ba_{1.553}UO_{3.866}$ ($= Ba_{1.205}U_{0.776}O_3$) for which we calculate from the X-ray data the values 8.135 and 7.563 g/cm^3, respectively, which are to be compared with the experimentally determined values (8.08 ± 0.03) and (7.55 ± 0.03) g/cm^3, respectively.

The perovskite-type barium uranate "$BaUO_3$" and its solid solutions with strontium differ considerably from the perovskite-type strontium uranate. In the latter case, the "$SrUO_3$" phase was shown to be not stable (4), and stabilization of the uranate is only possible in the presence of oxygen by oxidation of U^{4+} to U^{5+} via defect chemical reactions to give a phase with the discrete composition $Sr_2(Sr_{2/3}U_{1/3})UO_6$ (or $Sr_2UO_{4.5}$), which is structurally related to $Sr_3UO_6 (= Sr_2(Sr)UO_6)$ (19), however, with only 2/3 Sr per unit cell on a B site. At the same time a slight tilting of the UO_6 octahedra occurs which reduces the size of the cavity which is occupied by the alkaline-earth metal ions.

TABLE 4b
Atomic Distances (Å) and Angles (°) in $Ba_2(Ba_{0.414}U_{0.554})UO_6$ at Room Temperature

Ba–O(1)	2.806(10) 3×	U–O(1)	2.146(5) 6×
Ba–O(1)	3.121(28) 3×	Ba(2)/U(2)–O(1)	2.347(5) 6×
Ba–O(1)	3.190(23) 3×		

Whereas the $Sr_2UO_{4.5}$ phase has a discrete composition, the situation in "$BaUO_3$" is totally different. Again, stabilization of $BaUO_3$ occurs by oxidation of U^{4+} ions via the formation of metal vacancies rather than oxygen interstitials, but now Ba is *gradually* placed in the U vacancies on the B site. In the Kröger–Vink notation,

$$BaUO_3 + \frac{x}{2}O_2 = Ba_{1-y}\square''_{\frac{x}{3}+y}\left(U^{\times}_{1-2x}U^{\bullet}_{2x}Ba''_{y}\square''''_{\frac{x}{3}-y}\right)O_{3+x}$$

$$= \frac{3+x}{3}\left[Ba^{\times}_{\frac{3-3y}{3+x}}\square''_{\frac{x+3y}{3+x}}\left(U^{\times}_{\frac{3-6x}{3+x}}U^{\bullet}_{\frac{6x}{3+x}}\,Ba''_{\frac{3y}{3+x}}\,\square''''_{\frac{x-3y}{3+x}}\right)O_3\right]$$

or

$$Ba^{2+} + \frac{3}{2}O_2(g) + 6U^{4+} = Ba^{2+}_{U} + 2\square_{Ba} + 6U^{5+} + 3O^{2-}.$$

Although other defect mechanisms are possible, our neutron diffraction analysis and those by Barrett *et al.* (6), as well as lattice minimization calculations by Ball (20), suggest that the defect chemistry is dominated by anti-site disorder and that the process of moving a lattice A ion into uranium vacancies is energetically favorable.

From the experiments listed in Table 1 it follows that $BaUO_3$ is able to take BaO into solid solution up to a

TABLE 5b
Atomic Distances (Å) and Angles (°) in $Ba_{0.92}Sr_{0.08}(Sr_{0.13}U_{0.87})O_3$ at Room Temperature

Ba/Sr–O(1)	2.677(19)	U–O(1)	2.249(3)
–O(1)	2.935(14)	–O(2)	2.232(9)
–O(1)	3.367(14)	–O(2)	2.243(9)
–O(2)	2.798(12) 2×	O(1)–U–O(2)	90.6(33)
–O(2)	2.969(12) 2×	O(1)–U–O(2)	90.0(33)
–O(2)	3.153(18) 2×	O(2)–U–O(2)	91.3(32)
		U–O(1)–U	155.7(6)
		U–O(2)–U	159.7(4)

TABLE 6
Molar Enthalpy of Solution of a Mass *m* of $Ba_{1+y}UO_{3+x}$ in 250 cm³ $(HCl+0.0400FeCl_3+70.68H_2O)$ at 298.15 K

m(g)		εΘ (J)	ΔΘ	$\Delta_{sol}H_m$ (kJ mol^{-1})	Ba/U ratio
			a. $Ba_{1.033}UO_{3.134}$		
0.10635		120.5281	0.5426	− 264.441	
0.10390		118.7923	0.5372	− 264.124	
0.10497		119.7415	0.5409	− 265.335	
			mean:	− 264.63 ± 0.73	
			b. $Ba_{1.065}UO_{3.172}$		
0.11443		119.4770	0.6156	− 279.618	
0.11512		122.4086	0.6076	− 281.061	
0.10784		120.7086	0.5752	− 280.091	
			mean:	− 280.26 ± 0.85	
			c. $Ba_{1.238}UO_{3.407}$		
0.10541		120.4779	0.5656	− 299.015	
0.10572		119.8305	0.5733	− 300.573	
0.10398		118.9405	0.5627	− 297.725	
			mean:	− 299.10 ± 1.65	
			d. $Ba_{1.400}UO_{3.604}$		
0.10780		119.4450	0.5985	− 323.584	
0.10486		118.7794	0.5896	− 325.884	
0.10364		120.6702	0.5707	− 324.231	
			mean:	− 324.57 ± 1.37	
			e. $Ba_{1.553}UO_{3.866}$		
0.10573		120.1681	0.5751	− 335.412	
0.10356		119.9638	0.5659	− 336.390	
0.10594		119.6386	0.5778	− 334.838	
			mean:	− 335.55 ± 0.91	
			f. $BaCl_2$ UCl_4		
0.05168	0.08982	119.6323	0.3911	− 197.863	1.0495
0.06473	0.07431	120.2788	0.3309	− 203.441	1.5890
0.04337	0.09512	117.3773	0.4177	− 195.784	0.8317
0.07101	0.06791	118.3587	0.3119	− 206.482	1.9074
0.06871	0.07404	119.2078	0.3339	− 204.200	1.6928
0.08342	0.06108	120.5713	0.2841	− 213.018	2.4913
0.05269	0.07607	121.0748	0.3317	− 200.533	1.2635
0.05261	0.06294	117.6739	0.2872	− 203.957	1.5247
0.08435	0.06665	117.3116	0.3146	− 210.329	2.3085

TABLE 8
The Enthalpies of Formation at 298.15 K of Barium Uranates

Compound	Molar ratio U^{5+}/U	$\Delta_f H°$(298.15 K) (kJ mol^{-1})	Reference
$BaUO_{3.05}$	0.10	− 1700.4 ± 3.1	
$BaUO_{3.08}$	0.16	− 1710.0 ± 3.0	
$Ba_{1.033}UO_{3.134}$	0.20	− 1741.4	
$Ba_{1.065}UO_{3.172}$	0.21	− 1754.4	
$Ba_{1.238}UO_{3.407}$	0.34	− 1902.0	
$Ba_{1.400}UO_{3.604}$	0.41	− 2023.6	
$Ba_{1.553}UO_{3.866}$	0.63	− 2182.2	
$Ba_2U_2O_7$	1.0	− 3739.8	15
Ba_3UO_6	—	− 3210.7	17

maximum composition of approximately $Ba/U > 2.0$. As shown in Fig. 1 the volume of the unit cell gradually increases with the BaO content until maximum solubility is reached. Then BaO is present as the secondary phase, and no indications for the oxide Ba_3UO_5, as suggested by Charvillat *et al.* (7), have been found. The saturation concentration of BaO in the $BaUO_3$ structure depends on the oxygen pressure which governs the uranium vacancies. Finally, with increasing oxygen potential, e.g., in a H_2O/H_2 atmosphere, the pentavalent uranate $Ba_2U_2O_7$ will be formed, in agreement with observations by Braun *et al.* (8).

The solution of BaO into $BaUO_3$ can occur either substitutionally or interstitially with charge compensation through either vacancy or interstials, and a variety of defect schemes can be formulated. Again, lattice minimization calculations clearly show that the preferred method of solution involves the substitution of Ba into the barium and uranium sites in the $BaUO_3$ structure (20), with charge compensation through anion vacancies (half an oxygen vacancy per *A*O formule unit dissolved), ultimately resulting in a phase of composition $Ba_2(Ba, U)O_6$. Stabilization of

TABLE 7
Reaction Scheme for the Standard Molar Enthalpy of Formation of $Ba_{1.033}UO_{3.134}$(s) at the Temperature 298.15 K

Reaction		$\Delta_{sol}H^\circ_m$(kJ mol^{-1})
1. $Ba_{1.033}UO_{3.134}(s) + (2.268HCl + 1.798FeCl_3)(sln)$	$= (1.033BaCl_2 + UO_2Cl_2 + 1.798FeCl_2 + 1.134H_2O)(sln)$	− 264.63 ± 0.73
2. $1.033BaCl_2(s) + 0.899UCl_4(s) + (1.798\ FeCl_3 + 1.798H_2O)(sln)$	$= (1.033BaCl_2 + 0.899UO_2Cl_2 + 1.798FeCl_2 + 3.596HCl)(sln)$	− 199.13 ± 0.24
3. $0.101UO_2Cl_2(s) + sln$	$= 0.101UO_2Cl_2(sln)$	− 10.32 ± 0.06
4. $1.033Ba(s) + 1.033Cl_2(g)$	$= 1.033BaCl_2(s)$	− 883.37 ± 1.79
5. $0.101U(s) + 0.101O_2(g) + 0.101Cl_2(g)$	$= 0.101UO_2Cl_2(s)$	− 125.59 ± 0.13
6. $0.899U(s) + 1.798Cl_2(g)$	$= 0.899UCl_4(s)$	− 915.90 ± 2.25
7. $2.932H_2(g) + 2.932Cl_2(g) + sln$	$= 5.864HCl(sln)$	− 966.33 ± 0.53
8. $2.932H_2(g) + 1.466O_2(g) + sln$	$= 2.932H_2O(sln)$	− 838.09 ± 0.12
9. $1.033Ba(s) + U(s) + 1.567O_2(g)$	$= Ba_{1.033}UO_{3.134}(s)$	− 1741.44 ± 3.03

Note. $\Delta H9 = -\Delta H1 + \Delta H2 + \Delta H3 + \Delta H_4 + \Delta H5 + \Delta H6 - \Delta H7 + \Delta H8$. (sln) refers to $(HCl + 0.040FeCl_3 + 70.68\ H_2O)$.

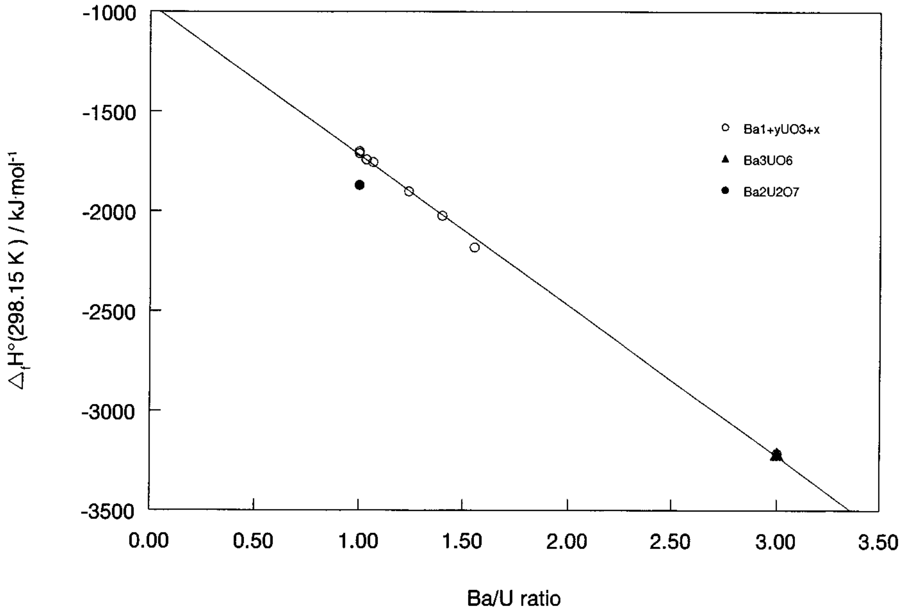

FIG. 3. The relationship between enthalpy of formation and the Ba/U ratio in $Ba_{1+y}UO_{3+x}$ at 298.15 K.

the $BaUO_3$-phase that occurs via oxidation of U^{4+} to U^{5+}, the creation of vacancies on the U sites in the lattice, and the simultaneous placement of Ba ions in the U vacancies, which ultimately leads to the Ba_3UO_6 structure ($= Ba_2(Ba, U)O_6$), in which U is in the hexavalent state, or Ba_2SrUO_6 (21). The system $Ba_2(Ba_xU_{1-x})UO_6$ is analogous to the system $Ba_2(Ba_xBi_{1-x})BiO_6$ (22). The end number $x = 0$ ($Ba_2Bi(III)Bi(V)O_6$) has a monoclinic structure at room temperature but above > 405 K it transforms to a rhombohedral structure. When additional barium atoms are introduced into the structure, substitution of Ba for Bi(III) occurs to give a rhombohedral structure.

It is interesting to note that SrO also dissolves in the "$BaUO_3$" structure, however, with a small decrease in the cell volume (Fig. 1 and Table 2), which follows from the ion sizes in the 12 coordination [Ba^{2+} 1.75 Å, Sr^{2+} 1.44 Å]

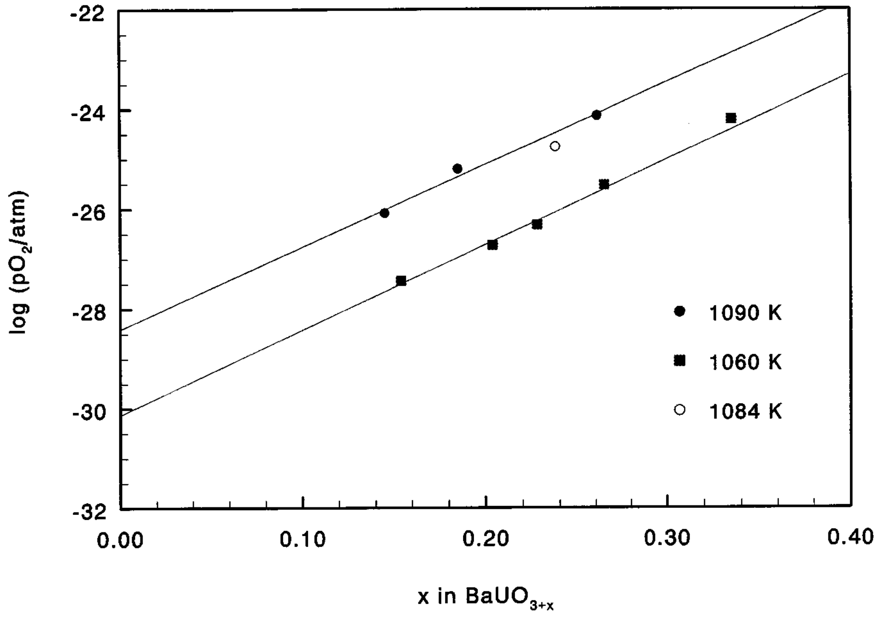

FIG. 4. Variation of oxygen potential with x in $Ba_{1.033}UO_{3+x}$ at two different temperatures.

TABLE 9
EMF Measurements vs Composition for $Ba_{1.033}UO_{3+x}$

Temperature (K)	Composition (x in $Ba_{1.033}UO_{3+x}$)	EMF (mV)	$\log pO_2$(atm)
1060	0.154	1407.0	−27.44
1060	0.204	1368.3	−26.73
1060	0.228	1346.8	−26.32
1060	0.265	1304.7	−25.53
1060	0.335	1202.6	−23.59
1084	0.238	1293.5	−24.76
1090	0.145	1371.1	−26.1
1090	0.185	1327.6	−25.3
1090	0.261	1268.0	−24.1

compared with U^{5+}(0.76 Å) (23). Again, its solubility depends on the oxygen potential.

When the enthalpies of formation at 298.15 K of $Ba_{1+y}UO_{3+x}$ (Table 8) are plotted as a function of y, a linear relationship is obtained (Fig. 3). As expected, $\Delta_f H^\circ(Ba_3UO_6)$ is a point on this line, being a member of the perovskite series $BaUO_3$–$Ba_{1+y}UO_{3+x}$–Ba_3UO_6. In contrast, $Ba_2U_2O_7$, in which U is pentavalent, is not a member of this series, having a different crystal structure (24).

5. CONCLUSIONS

The perovskite-type $BaUO_3$ structure has been investigated by X-ray and neutron diffraction, using samples in which the Ba/U ratio, (Ba, Sr)/U ratio, and the oxygen stoichiometry in $Ba_{1+y}UO_{3+x}$ were varied. In addition, thermodynamic properties of these samples, the integral enthalpies of formation and the equilibrium oxygen partial pressure, were measured. It is concluded that the continuous series $BaUO_3$–$Ba_{1+y}UO_{3+x}$–Ba_3UO_6 exists in which the uranium vacancies are gradually filled with barium ions whereas uranium is oxidized via the pentavalent to the hexavalent state in Ba_3UO_6.

REFERENCES

1. H. Kleykamp, J. O. Paschoal, R. Pesja, and F. Thümmler, *J. Nucl. Mater.* **130,** 426 (1985).
2. H. Kleykamp, *J. Nucl. Mater.* **131,** 221 (1985).
3. H. Kleykamp, *J. Nucl. Mater.* **206,** 82 (1993).
4. E. H. P. Cordfunke and D. J. W. IJdo, *J. Solid State Chem.* **109,** 272 (1994).
5. C. W. Williams, L. R. Morss, and In-Kyu Choi, “ACS Symposium Series,” No. 246, p. 323. Am. Chem. Soc., Washington, DC, 1984.
6. S. A. Barrett, A. J. Jacobson, B. C. Tofield, and B. E. F. Fender, *Acta Crystallogr. B* **38,** 2775 (1982).
7. J. P. Charvillat, G. Baud, and J. P. Besse, *Mater Res. Bull.* **5,** 933 (1970).
8. R. Braun, S. Kemmler-Sack, H. Roller, I. Seemann, and I. Wall, *Z. Anorg. Allg. Chem.* **415,** 133 (1975).
9. H. M. Rietveld, *J. Appl. Crystallogr.* **2,** 65 (1969).
10. K. Weber, *Acta Crystallogr.* **23,** 720 (1967).
11. F. Sears, *Neutron News* **3,** 26 (1992).
12. D. B. Wiles and R. A. Young, *J. Appl. Crystallogr.* **14,** 149 (1981).
13. E. H. P. Cordfunke, W. Ouweltjes, and G. Prins, *J. Chem. Thermodynam.* **7,** 1137 (1975).
14. G. G. Cristoph, A. C. Larson, P. G. Eller, J. D. Purson, J. D. Zahrt, R. A. Penneman, and G. H. Rinnehart, *Acta Crystallogr. B* **44,** 575–580 (1988).
15. E. H. P. Cordfunke and W. Ouweltjes, *J. Chem. Thermodynam.* **20,** 235–238 (1988).
16. E. H. P. Cordfunke, R. J. M. Konings, and W. Ouweltjes, *J. Chem. Thermodynam.* **22,** 991 (1990).
17. “Thermochemical Data for Reactor Materials and Fission Products,” E. H. P. Cordfunke and R. J. M. Konings (Eds.), p. 72–73. Amsterdam, 1990.
18. M. Yamawaki, J. Huang, K. Yamaguchi, M. Yasumoto, H. Sakurai, and Y. Susuki, *J. Nucl. Mater.* **231,** 199–203 (1996).
19. D. J. W. IJdo, *Acta Crystallogr. Sect. C* **49,** 650 (1993).
20. R. G. J. Ball, *J. Mater. Chem.* **2,** 641 (1992).
21. W. A. Groen and D. J. W. IJdo, *Acta Crystallogr. C* **43,** 1033–1036 (1987).
22. K. P. Reis, A. J. Jacobson, and J. M. Nichol, *J. Solid State Comm.* **107,** 428–443 (1993).
23. R. D. Shannon, *Acta Crystallogr. A* **32,** 751 (1976).
24. E. H. P. Cordfunke and D. J. W. IJdo, *J. Phys. Chem. Solids* **49,** 551–554 (1988).